AIP | Applied Physics Letters

High-resolution single-mode fiber-optic distributed Raman sensor for absolute temperature measurement using superconducting nanowire single-photon detectors

Michael G. Tanner, Shellee D. Dyer, Burm Baek, Robert H. Hadfield, and Sae Woo Nam

Citation: Appl. Phys. Lett. **99**, 201110 (2011); doi: 10.1063/1.3656702
View online: http://dx.doi.org/10.1063/1.3656702
View Table of Contents: http://apl.aip.org/resource/1/APPLAB/v99/i20
Published by the American Institute of Physics.

High-resolution single-mode fiber-optic distributed Raman sensor for absolute temperature measurement using superconducting nanowire single-photon detectors

Michael G. Tanner,[1,a)] Shellee D. Dyer,[2] Burm Baek,[2] Robert H. Hadfield,[1] and Sae Woo Nam[2]
[1]*Scottish Universities Physics Alliance and School of Engineering and Physical Sciences, Heriot-Watt University, Edinburgh EH14 4AS, United Kingdom*
[2]*National Institute of Standards and Technology, Optoelectronics Division, Boulder, Colorado 80305, USA*

(Received 7 July 2011; accepted 5 October 2011; published online 17 November 2011)

We demonstrate a distributed fiber Raman sensor for absolute temperature measurement with spatial resolution on the order of 1 cm at 1550 nm wavelength in a single-mode fiber using superconducting nanowire single-photon detectors. Rapid measurements are shown, with less than 60 s integration period, allowing the demonstration of temperature evolution in an optical fiber recorded at over 100 resolvable, 1.2 cm spaced positions along the fiber simultaneously. This distributed sensor has potential application as a primary reference standard, in which high-accuracy, high-spatial-resolution temperature measurements can be obtained without the need for a separate temperature calibration standard. © *2011 American Institute of Physics*. [doi:10.1063/1.3656702]

Distributed fiber-optic sensors are an attractive alternative to multiplexed point sensors, because a single fiber-optic cable can potentially replace thousands of individual sensors and dramatically simplifying sensor installation and readout. Two important classes of distributed fiber optic sensors are coherent optical frequency-domain reflectometry (OFDR)[1] and optical time-domain reflectometry (OTDR).[2] Coherent OFDR systems have the advantage of high spatial resolution (on the order of 1 cm)[1] and good temperature resolution (on the order of 1 K), but the maximum sensing range is generally limited to 10 m.

OTDR measurements typically employ a pulsed source and determine position information from the time-of-flight of the photons that are backscattered from the fiber under test (FUT). One important class of OTDR sensors is based on the measurements of Raman scattering. Dakin *et al.* were the first to demonstrate that the temperature could be determined from a ratio of measured Stokes and anti-Stokes Raman scattering.[2] Typical performance of a Raman-based OTDR is 1 m spatial resolution and 1 K accuracy for a 5-min measurement integration period, with a system range of 10 km.[3] The range is typically limited by loss in the fiber and fiber intermodal dispersion (if multimode fiber is used as the sensing fiber). Another factor affecting OTDR range is the pulse rate of the pump laser, but this can be modulated, either internally or externally to the pump laser. The 1 m spatial resolution that is typical for Raman-based OTDR sensors is sufficient for some commercial applications, such as monitoring of oil and gas wells, but there are other applications, such as the detection of hot spots along the steam pipes of power plants, where spatial resolution much better than 1 m is required.[4]

One drawback of distributed-fiber sensors is that the backscattered signal is typically very weak; therefore, early work focused on multimode fibers to increase the collection of backscattered photons. Additionally, pump lasers near 800 nm–900 nm were chosen so that high-performance silicon avalanche photodiodes (APDs) could be used for detection.[2]

In this paper, we demonstrate a distributed temperature sensor with very high spatial resolution using a single-mode FUT, operating in the telecom C-band with wavelengths near 1550 nm. We employ time-correlated single-photon counting techniques,[4,5] in which we create histograms of the time delays between the launch of a laser pulse and the detection of backscattered photons at our superconducting nanowire single-photon detectors (SNSPDs). These detectors have exceptional performance in the visible to mid-infrared wavelength regions[6,7] and can be integrated into practical closed-cycle refrigerator-based detector systems[8] for use in advanced photon-counting experiments. The low timing jitter of the SNSPDs allows us to achieve spatial resolution on the order of 1 cm in standard single-mode telecommunications fiber.

A diagram of our measurement setup is shown in Fig. 1. The entire system is constructed from inexpensive, standard, off-the-shelf fiber-optic components that were designed for the telecommunication industry. The sensing fiber is a standard single mode fiber with a mode field diameter of 10.4 μm and attenuation less than 0.2 dB/km at a wavelength of

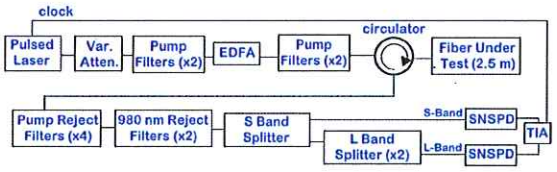

FIG. 1. (Color online) Diagram of our high-spatial-resolution fiber-optic temperature-sensor system. The pulsed laser is a femtosecond fiber laser with a 36 MHz clock rate. The pump filters are bandpass filters with 1 nm linewidth at a center wavelength of 1533.47 nm. The pump rejection filters are identical to the pump filters, but are connected so that they reject the pump wavelength and pass all other wavelengths. The bandsplitters are used to separate the S-band wavelengths (1460 nm–1490 nm) and L-band wavelengths (1570 nm–1610 nm) from the C-band wavelengths (1530 nm–1565 nm). EDFA: erbium-doped fiber amplifier, SNSPD: superconducting-nanowire single-photon detector, TIA: time-interval analyzer.

a)Electronic mail: M.Tanner@hw.ac.uk.

1550 nm. Our source is a femtosecond fiber laser with a repetition frequency of 36 MHz and a spectrum centered near 1550 nm. We apply a 1 nm linewidth bandpass filter to the pump laser. We also attenuate the pump laser before amplifying it with an erbium-doped fiber amplifier (EDFA). The attenuator minimizes the pulse distortion due to gain saturation in the EDFA. We use 1-nm wide bandpass filters post-amplification to remove all broadband amplified spontaneous emission (ASE) from the pump, which could otherwise be Rayleigh backscattered in the FUT, and create unwanted counts at our detectors. We apply multiple filters in series both before and after the EDFA, because each filter typically provides 20-30 dB rejection of unwanted wavelengths. We inject the pump light into our FUT via a fiber-optic circulator. The length of our FUT is currently limited to about 2.8 m by the repetition rate of our pump laser. The light that is backscattered from the FUT is directed by the circulator to a series of filters that have been chosen to reject the pump wavelength. Without these filters, we would have unwanted photons at the pump wavelength reaching our detector due to Rayleigh backscattering in the FUT, Fresnel reflection at the endface of the FUT, and imperfections in the circulator and imperfections of the fiber-to-fiber interconnections. The far endface of the FUT is immersed in index-matching fluid to further suppress Fresnel reflections at that endface. The 980 nm filters are used to block any of the EDFA pump photons that might otherwise reach the detectors. We use a series of band splitters to separate and filter the Raman-backscattered photons into an S-band channel (1460 nm–1490 nm) and a L-band channel (1570 nm–1610 nm). The pump wavelength was chosen to be 1533.47 nm (ITU Channel 55), so that it was approximately equally spaced between the S- and L-bands. The time-interval analyzer (TIA) creates histograms of the time delays between a laser clock electrical pulse and the electrical pulses created by the detection of photons at the SNSPDs.

We model the Stokes and anti-Stokes contributions to the total Raman backscattering as follows:[9]

$$I_u \approx \eta_u \Delta\nu_u P_0 L |g_R| N(\Omega_{up}) D_c, \tag{1}$$

where I_u is the backscattered photons per second, the subscript u is either S or a for Stokes or anti-Stokes, η_u is the detection efficiency (DE) of the SNSPDs, $\Delta\nu_u$ is the bandwidth of the Stokes or anti-Stokes filters, P_0 is the peak pump power, L is fiber length, g_R is the Raman gain factor, D_c is the duty cycle of the pump signal, Ω_{up} is the radial frequency detuning between the pump and the mean Stokes or anti-Stokes wavelengths, and N represents the phonon population as follows:

$$N \approx \begin{cases} \dfrac{1}{\exp\left(\dfrac{\hbar|\Omega_{up}|}{k_B T}\right) - 1} & \text{when} \quad \Omega_{up} > 0 \\ \dfrac{1}{\exp\left(\dfrac{\hbar|\Omega_{up}|}{k_B T}\right) - 1} + 1 & \text{when} \quad \Omega_{up} < 0. \end{cases} \tag{2}$$

The Raman gain generally increases with detuning, reaching a peak near a detuning of 15 THz (approximately 100 nm), but is typically quite small, i.e., on the order of $1.0\,\mathrm{W^{-1}\cdot km^{-1}}$. Although SNSPDs with high detection efficiency have been demonstrated,[10,11] the devices available for this project had relatively low DEs on the order of 1%.[7] Our pump power is limited by gain saturation in our EDFA to around $P_{ave} = 18$ mW. Therefore, we maximized our output power with wide Stokes and anti-Stokes filters and detunings that were as large as possible (while still using standard telecom components). This configuration achieved count rates of approximately 2×10^5 Hz on each channel at room temperature, near the maximum acceptable without pulse pile-up causing distortion of measured data.

If we approximate the Raman gain g_R and detuning Ω_{up} as constant over our Stokes and anti-Stokes filter bandwidths, and assume $\Omega_{ap} \approx \Omega_{sp}$, then the ratio of Stokes to anti-Stokes is given by

$$\frac{I_s(x) - B_s}{I_{as}(x) - B_{as}} \approx \frac{\eta_s \Delta\nu_s |g_{R,s}|}{\eta_a \Delta\nu_a |g_{R,a}|} \exp\left(\frac{\hbar|\Omega_{sp}|}{k_B T(x)}\right) \approx C \exp\left(\frac{\hbar|\Omega_{sp}|}{k_B T(x)}\right), \tag{3}$$

where I_s is the Stokes counts, B_s is the Stokes background counts (from dark counts and Rayleigh-backscattered ASE), I_{as} is the anti-Stokes counts, B_{as} is the anti-Stokes background counts, x is the position in the FUT, and C is a constant, which includes the detection efficiency of the two SNSPDs, relative Raman gain, and width of the two detection bands. If a short section of our sensing fiber is held at a known temperature, we are able to determine C using that section. We then calculate the temperature of the entire fiber as a function of position from our measured histogram data, using Eq. (3).

Although we find it convenient to determine C from measured data at a known temperature, it is theoretically possible to obtain C through a careful characterization of detection efficiencies, Raman gain profiles, and spectral responses of the detection filters. This creates the potential to apply this thermometer as a primary standard, in which the temperature measurements of high accuracy can be obtained without the need for any type of temperature calibration reference.

We demonstrated the high spatial resolution of our sensor as follows. We manufactured a defect region in an electrical wire by soldering a short (approximately 12 mm) section of narrow-gauge wire in series with a wire of thicker gauge. The total length of the electrical wire was approximately 2 m, to match the length of our fiber under test. We wrapped the sensor fiber around the electrical wire, so that the fiber was in close proximity with the electrical wire throughout its length and applied approximately 2 A of current to the electrical wire. Fig. 2 shows the temperature of the fiber determined from a 10 min integration period. The defect section of the electrical wire creates a localized hot spot, which is clearly evident from the temperature measurement shown in Fig. 2. The FWHM timing jitter of our system is approximately 85 ps; this total includes the jitter of both detectors, the laser, and the triggering electronics. This corresponds to approximately 9 mm spatial resolution. If we were able to apply a heating as a delta function profile at a single point on the fiber, we would expect to recover this resolution in our measurement. However, a Gaussian response with 12 mm FWHM is observed in Fig. 2 when heat from the wire defect is applied to the sensing fiber. We believe the observed width

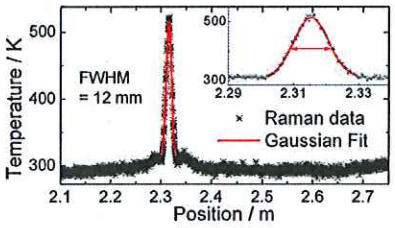

FIG. 2. (Color online) Results of the temperature measurement from an electrical wire with a short (approximately 12 mm) defect section of narrow-gauge electrical wire in series with a thicker-gauge wire. When current is applied to the electrical wire, the defect section is heated, and we are able to measure that temperature spike with our sensing system. A histogram bin size of 4 ps was used, with an integration period of 10 min.

is consistent with a convolution of the system response and the temperature distribution due to the applied heat.

We also demonstrated the potential for rapid measurement of temperature evolution as follows. Three loops, each with a diameter of approximately 11 cm, were created from a section of our FUT. Approximately half of each loop was submerged into a hot water bath and temperature was measured in 1 min intervals over the course of an hour as the water bath cooled. The result is shown in Fig. 3(a), where we show the temperature (vertical axis) as a function of position in the fiber, with the second horizontal axis showing the relative time at which each measurement was performed as the water bath was cooled. For comparison, we simultaneously measured the water bath temperature with a thermocouple; Fig. 3(b) compares the temperatures measured with the fiber sensor and thermocouple.

We have demonstrated a distributed fiber-optic temperature sensor based on Raman scattering with very high spatial resolution, enabled by the low timing jitter of the SNSPDs (on the order of 60 ps), which results in spatial resolution on the order of 1 cm. Early demonstrations of distributed temperature sensors used multimode fiber to increase the collection efficiency of the Raman scattered photons, but spatial resolution was limited by the modal dispersion of the fiber as well as the timing performance of the detectors. In this paper, we demonstrate a sensing system using standard low-loss telecom single-mode optical fiber. Our system efficiency is determined by the choice of filters and fiber components, as well as by the detection efficiency of our SNSPDs. Our Raman scattering collection efficiency is so high that accurate temperature measurements can be obtained in less than 1 min integration period. We expect that this technique could be applied to long-range distributed sensors, because it is compatible with telecommunications-grade single-mode fiber, in which intermodal dispersion and fiber loss are minimized. Fiber length in the current experiment was limited to ~2.8 m by the laser pulse frequency (36 MHz). A repetition rate of 0.1 MHz would allow a fiber length of 1 km without crosstalk between the subsequent pulses. At the same pulse energy, count rates would drop by a factor of 400 (including 0.2 dB/km attenuation). The authors have previously demonstrated practical fiber coupled SNSPDs at 1550 nm with ten times greater efficiency than those in this experiment.[11] Using these detectors with a factor of 40 increased pulse energy of the pump (corresponding to an average power of just 2.0 mW), a 1 km range distributed sensor, with the count rates and rapid measurement characteristics described in this paper, is possible. We plan to detail the measurement uncertainties in a future paper.[12]

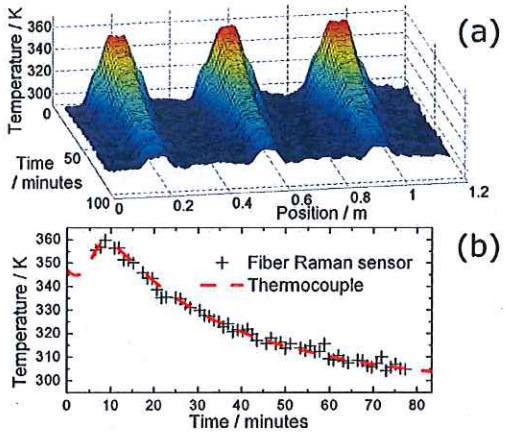

FIG. 3. (Color online) (a) Plot of measured temperature from a fiber that was coiled into three loops with 11 cm diameter and partially immersed in a hot water bath. The vertical axis shows the measured temperature of the fiber, the first horizontal axis shows the position along the fiber, and the second horizontal axis shows time as the water bath was allowed to cool. Measurements were taken in 1-min intervals (1-min integration period) as the water bath cooled. Peaks in temperature are seen at the expected 35 cm spacing. (b) Comparison of temperature measured with the fiber Raman sensor from one peak and a conventional thermocouple. A reference temperature of 295 K was used for the section of the fiber at room temperature, and the detuning of 59 nm between pump and Stokes/anti-Stokes bands was applied to process the Raman data. The time-stamps for both data sets of (b) were recorded in the experiment; there are no free parameters in the comparison shown in (b). Plotted data have a 5-point adjacent average applied along the spatial (position) axis [for (b) the 5 adjacent points averaged are all at the same temperature, immersed in the bath].

The authors are grateful to the National Institute of Information and Communications Technology (NICT) of Japan for providing SNSPDs for this experiment. M.G.T. and R.H.H. acknowledge funding from the UK Engineering and Physical Sciences Research Council. R.H.H. also acknowledges a Royal Society University Research Fellowship. The authors thank Robert Maier and Bill MacPherson for useful discussions.

[1]S. T. Kreger, D. K. Gifford, M. E. Froggatt, B. J. Soller, and M. S. Wolfe, *Optical Fiber Sensors*, OSA Technical Digest (CD) (Optical Society of America, 2006), Paper ThE42.
[2]J. P. Dakin and D. J. Pratt, Electron. Lett. **21**, 569 (1985).
[3]L. Thévenaz, "Review and Progress on Distributed Fibre Sensing," in *Optical Fiber Sensors*, OSA Technical Digest (CD) (Optical Society of America, 2006), Paper ThC1.
[4]R. Feced, M. Farhadiroushan, V. A. Handerek, and A. J. Rogers, IEE Proc.: Optoelectron. **144**, 183 (1997).
[5]R. Stierlin, J. Ricka, B. Zysset, R. Bättig, H. P. Weber, T. Binkert, and W. J. Borer, Appl. Opt. **26**, 1368 (1987).
[6]R. H. Hadfield, Nature Photon. **3**, 696 (2009).
[7]S. Miki, M. Fujiwara, M. Sasaki, B. Baek, A. J. Miller, R. H. Hadfield, S. Nam, and Z. Wang, Appl. Phys. Lett. **92**, 061116 (2008).
[8]R. H. Hadfield, M. J. Stevens, S. G. Gruber, A. J. Miller, R. E. Schwall, R. P. Mirin, and S. W. Nam, Opt. Express **13**(26), 10846 (2005).
[9]Q. Lin, F. Yaman, and G. P. Agrawal, Phys. Rev. A **75**, 023803 (2007).
[10]K. M. Rosfjord, J. K. W. Yang, E. A. Dauler, A. J. Kerman, V. Anant, B. M. Voronov, G. N. Gol'tsman, and K. K. Berggren, Opt. Express **14**(2), 527 (2006).
[11]M. G. Tanner, C. M. Natarajan, V. K. Pottapenjara, J. A. O'Connor, R. J. Warburton, R. H. Hadfield, B. Baek, S. Nam, S. N. Dorenbos, E. Bermudez Urena, T. Zijlstra, T. M. Klapwijk, and V. Zwiller, Appl. Phys. Lett. **96**, 221109 (2010).
[12]S. D. Dyer, M. G. Tanner, B. Baek, R. H. Hadfield, and S. W. Nam, "Analysis of a distributed fiber-optic temperature sensor using single-photon detectors," Optics Express (submitted).